Contribution from the Departament de Química Inorgànica, Facultat de Química, and Departament de Cristal.lografia, Mineralogia i Dipòsits Minerals, Facultat de Geologia, Universitat de Barcelona, Diagonal 647, 08028 Barcelona, Spain

Synthesis and Study of the Fluxional Behavior of Octahedral Manganese(I) Complexes with a Monodentate 1,8-Naphthyridine Ligand. X-ray Crystal Structure of *fac*-[Mn(η^1-1,8-naph)(η^2-phen)(CO)$_3$]ClO$_4$·$^1/_2$CH$_2$Cl$_2$ (naph = 1,8-Naphthyridine, phen = *o*-Phenanthroline)

María-José Bermejo,† José-Ignacio Ruiz,† Xavier Solans,‡ and Jordi Vinaixa*,†

Received March 24, 1988

The addition of 1,8-naphthyridine (naph) to a solution of [Mn(OClO$_3$)(chel)(CO)$_3$] (chel = *o*-phenanthroline (phen), 2,2′-bipyridyl (bpy)) affords the octahedral complexes [Mn(η^1-naph)(η^2-chel)(CO)$_3$]ClO$_4$. The crystal structure of [Mn(η^1-naph)(η^2-phen)(CO)$_3$]ClO$_4$·$^1/_2$CH$_2$Cl$_2$ (monoclinic, space group $P2_1/a$, a = 19.019 (4) Å, b = 16.120 (3) Å, c = 8.368 (2) Å, β = 90.68 (2)°, Z = 4) shows that in the complex ion the manganese atom displays a slightly distorted octahedral coordination, being linked to three carbonyl ligands in a *fac* position, to two nitrogen atoms of a bidentate *o*-phenanthroline ligand (η^2-phen), and to another nitrogen atom of a monodentate 1,8-naphthyridine ligand (η^1-naph). A detailed variable-temperature ^{1}H NMR study shows that this structure persists in solution at low temperature for both complexes. At higher temperature these complexes are fluxional species in which there is a rapid exchange of the site of manganese coordination between the two nitrogen atoms of the monodentate 1,8-naphthyridine. For this process an approximate activation energy of 63 kJ/mol has been obtained for both complexes. The mechanism for the 1,3-shift is, apparently, intramolecular and is such that the manganese–naphthyridine interaction is probably never lost during the process.

Introduction

Potentially bidentate 1,3-ligands[1] (1,3-L) are a very interesting class of ligands. Ligands of this type with the most common donor atoms (oxygen,[2] nitrogen,[3] sulfur,[4] phosphorus,[5] and selenium[4]) are known. Due to the donor atom lone-pair orientation, they can function either as monodentate (η^1-1,3-L) or bidentate (η^2-1,3-L) ligands to a single metal atom or as a bridging ligand between two metal atoms (μ_2-1,3-L). When monodentate, these ligands can undergo a dynamic process that renders both donor atoms equivalent in what can be called a 1,3-haptotropic shift.[6] Recently, we have become interested in the coordination behavior of 1,8-naphthyridine (naph) and in the study of its dynamic behavior when monodentate. This potentially bidentate 1,3-ligand is known to form monodentate complexes with most d^8 transition-metal ions that usually form square-planar complexes: Au(III),[7] Pt(II),[8] Pd(II),[9] Ni(II),[10] Ir(I),[11] and Rh(I).[11,12] This ligand has also been found to adopt a monodentate coordination in octahedral complexes of d^6 central atoms: Cr(0), Mo(0), and W(0)[13,14] and Fe(II).[15] For all the above-mentioned square-planar complexes, a dynamic behavior that renders both donor atoms of the monodentate naphthyridine equivalent has been found to occur. A similar behavior has been observed for the octahedral complexes [M(naph)(CO)$_5$] (M = Cr, Mo, and W),[13,14] while the pseudooctahedral Fe(II) complex [CpFe(CO)$_2$(naph)]$^+$ has been found to be rigid.[15]

In order to understand the dynamic behavior of the naph ligand when monodentate, we undertook molecular orbital calculations (extended Hückel, EH) on model systems. We found that for octahedral complexes the energy barrier for the 1,3-haptotropic shift very much depends on the appearance of a four-electron repulsion between the lone pairs and one of the metal's "t_{2g}" orbitals in the transition state. For this type of complexes, the height of the potential energy barrier is expected to be in the order Cr(0) < Mn(I) < Fe(II).[16] The experimental results for Cr(0)[14] and Fe(II)[15] were in accord with this energy sequence, but no comparison could be made with manganese(I) because no octahedral complex of this ion with monodentate 1,8-naphthyridine had been prepared. Thus, it seemed interesting to prepare and study complexes of this type.

Experimental Section

General Remarks. The reactions were carried out under dry nitrogen or argon, with use of Schlenk-tube techniques. Solvents were dried by appropriate methods and distilled under nitrogen prior to use. Chemical analyses were carried out at the "Institut de Química Bio-orgànica de Barcelona (CSIC)".

Conductivities of 10^{-4} M acetone solutions of the new compounds were measured with a Radiometer CMD3 conductivity bridge.

Proton NMR spectra were obtained from acetone-d_6 solutions and

Table I. Crystallographic Data for *fac*-[Mn(η^1-naph)(η^2-phen)(CO)$_3$]ClO$_4$·$^1/_2$CH$_2$Cl$_2$

chem formula: $C_{23}H_{14}ClN_4O_7Mn\cdot{}^1/_2CH_2Cl_2$	fw: 591.25
a = 19.019 (4) Å	space group: $P2_1/a$ (No. 14)
b = 16.120 (3) Å	T = 15 °C
c = 8.368 (2) Å	λ(Mo Kα) = 0.710 69 Å
β = 90.68 (2)°	ρ_{calc} = 1.530 g cm^{-3}
V = 2565.3 (9) Å^3	μ = 8.01 cm^{-1}
Z = 4	$R(F_o)$ = 0.061
	$R_w(F_o)$ = 0.068

† Departament de Química Inorgànica, Facultat de Química.
‡ Departament de Cristal.lografia, Mineralogia i Dipòsits Minerals, Facultat de Geologia.

(1) By potentially bidentate 1,3-ligands we refer to ligands with two donor atoms in 1,3 relative positions.
(2) Deacon, G. B.; Phillips, R. J. *Coord. Chem. Rev.* **1980**, *33*, 227.
(3) (a) Paudler, W. W.; Sheets, R. M. *Adv. Heterocycl. Chem.* **1983**, *33*, 147. (b) Toniolo, L.; Immirzi, A.; Croatto, U.; Bombieri, G. *Inorg. Chim. Acta* **1976**, *19*, 209 and references therein. (c) Baker, J.; Cameron, N.; Kilner, M.; Mahoud, M. M.; Wallwork, S. C. *J. Chem. Soc., Dalton Trans.* **1986**, 1359 and references therein.
(4) Abel, E. W.; Bhargava, S. K.; Orrell, K. G. *Prog. Inorg. Chem.* **1984**, *32*, 1.
(5) (a) Pringle, P. G.; Shaw, B. L. *J. Chem. Soc., Chem. Commun.* **1982**, 81; **1982**, 581 and references therein. (b) Hoffman, D. M.; Hoffmann, R. *Inorg. Chem.* **1981**, *20*, 3543 and references therein. (c) Puddephatt, R. J.; Thomson, M. A.; Manojlovic-Muir, L.; Muir, K. W.; Frew, A. A.; Brown, M. P. *J. Chem. Soc., Chem. Commun.* **1981**, 805 and references therein.
(6) Although commonly used in organometallic chemistry to describe the fluxional process of metal polyene complexes, the term "haptotropic rearrangement" describes in general the change in connectivity (η number) of a metal to a ligand with multicoordinated site possibilities: Anh, N. T.; Elian, M.; Hoffmann, R. *J. Am. Chem. Soc.* **1978**, *100*, 110. Albright, T. A.; Hofmann, P.; Hoffmann, R.; Lillya, C. P.; Dobosh, P. A. *J. Am. Chem. soc.* **1983**, *105*, 3396. See also ref 16.
(7) Schmidbaur, H.; Dash, K. C. *J. Am. Chem. Soc.* **1973**, *95*, 4855.
(8) Dixon, K. R. *Inorg. Chem.* **1977**, *16*, 2618.
(9) Brandon, J. B.; Collins, M.; Dixon, K. R. *Can. J. Chem.* **1978**, *56*, 950.
(10) Bermejo, M. J.; Vinaixa, J.; Pidcock, A.; Nowell, I. W., to be submitted for publication.
(11) Balch, A. L.; Copper, R. A. *J. Organomet. Chem.* **1979**, *169*, 97.
(12) Tiripicchio, A.; Tiripicchio-Camellini, M.; Usón, R.; Oro, L. A.; Ciriano, M. A.; Viguri, F. *J. Chem. Soc., Dalton Trans.* **1984**, 125.
(13) Reed, T. E.; Hendricker, D. G. *J. Coord. Chem.* **1972**, *2*, 83.
(14) Dixon, K. R.; Eadie, D. T.; Stobart, S. R. *Inorg. Chem.* **1982**, *21*, 4318.
(15) Bermejo, M. J.; Martinez, B.; Vinaixa, J. *J. Organomet. Chem.* **1986**, *304*, 207.
(16) Alvarez, S.; Bermejo, M. J.; Vinaixa, J. *J. Am. Chem. Soc.* **1987**, *109*, 5316.

0020-1669/88/1327-4385$01.50/0

were recorded on a Bruker WP 80SYFT spectrometer, equipped with a B-VT-1000 variable-temperature unit, and a Varian XL 200 spectrometer; chemical shifts were referenced to internal $SiMe_4$.

1,8-Naphthyridine(naph)[17] and the complex $[MnBr(phen)(CO)_3]$[18] (phen = *o*-phenanthroline) were prepared as previously described. $[MnBr(bpy)(CO)_3]$ (bpy = 2,2′-bipyridyl) was prepared by the same method as for the phen analogue.

Preparation of $[Mn(naph)(chel)(CO)_3]ClO_4$ (chel = *o*-Phenanthroline (1), 2,2′-Bipyridyl (2)). A mixture of $[MnBr(chel)(CO)_3]$ (chel = *o*-phenanthroline, 2,2′-bipyridyl; 1 mmol) and $AgClO_4$ (0.25 g, 1.2 mmol) in CH_2Cl_2 (75 mL) was stirred at room temperature for 3 h. The resulting solution of $[Mn(OClO_3)(chel)(CO)_3]$ was then filtered through Celite. 1,8-Naphthyridine (0.13 g, 1 mmol) was added to the solution, and after the mixture was stirred at room temperature for 3 h, diethyl ether (50 mL) was added. The microcrystalline solid was filtered, washed with diethyl ether and hexane, and then vacuum-dried; yield ca. 60%.

$[Mn(naph)(phen)(CO)_3]ClO_4$: mp 110–112 °C. Anal. Calcd for $C_{23}H_{14}ClMnN_4O_7$: C, 50.3; H, 2.6; N, 10.2. Found: C, 50.0; H, 2.6; N, 9.9. IR(CH_2Cl_2): ν_{max}(CO) 2060 s, 1965 s, 1950 s cm^{-1}. Λ_M = 150 Ω^{-1} cm^2 mol^{-1} (acetone). ^1H NMR (acetone-d_6, 293 K) δ_H(phen) 10.26 [2 H, dd, $J(\alpha\beta)$ = 5.2 Hz, $J(\alpha\gamma)$ = 1.2 Hz, H_α], 8.29 [2 H, dd, $J(\beta\gamma)$ = 7.8 Hz, H_β], 8.90 [2 H, dd, H_γ], 8.2 [2 H, s, H_δ].

$[Mn(naph)(bpy)(CO)_3]ClO_4$: mp 100–102 °C. Anal. Calcd for $C_{21}H_{14}ClMnN_4O_7$: C, 48.1; H, 2.7; N, 10.7. Found: C, 47.9; H, 2.7; N, 10.7. IR (CH_2Cl_2): ν_{max}(CO) 2044 s, 1960 s, 1943 s cm^{-1}. Λ_M = 141 Ω^{-1} cm^2 mol^{-1} (acetone). ^1H NMR (acetone-d_6, 293 K) δ_H(bpy) 9.84 [2 H, ddd, $J(\alpha\beta)$ = 6.0 Hz, $J(\alpha\gamma)$ = 1.5 Hz, $J(\alpha\delta)$ = 0.8 Hz, H_α], 7.93 [2 H, ddd, $J(\beta\gamma)$ = 7.2 Hz, $J(\beta\delta)$ = 1.4 Hz, H_β], 8.28 [2 H, td, $J(\gamma\delta)$ = 8.0 Hz, H_γ], 8.50 [2 H, ddd, H_δ].

Structure Determination of *fac*-$[Mn(\eta^1\text{-naph})(\eta^2\text{-phen})(CO)_3]ClO_4 \cdot {}^1/_2CH_2Cl_2$. A single crystal suitable for the X-ray diffraction study was grown by cooling a saturated CH_2Cl_2 solution of $[Mn(\eta^1\text{-naph})(\eta^2\text{-phen})(CO)_3]ClO_4$ at −15 °C for several weeks. The details of the crystal structure are given in Table I. The rest of the relevant information on the crystal data collection and refinement is collected in the supplementary material.

Safety Note. Even though we have not had any problems using perchlorate salts and perchlorate complexes, it must be borne in mind that perchlorate salts of metal complexes with organic ligands are potentially exposive.[19] Thus, great caution should be exercised when handling these materials.

Results and Discussion

Preparation and Characterization. It is well-known that pentacarbonyl complexes of the type $[MnL(CO)_5]^+$ (L = aromatic amine) easily decompose by losing carbonyl ligands, while the analogous tricarbonyl complexes of *fac* geometry are much more stable. As we wanted not only to synthesize an octahedral complex of manganese(I) with a monodentate naph ligand but also to study its variable-temperature ^1H NMR spectra, the preparation of a 1,8-naphthyridine complex was attempted, from the beginning, from an octahedral *fac*-tricarbonylmanganese(I) complex.

The room-temperature reaction between $[Mn(OClO_3)(chel)(CO)_3]$ (chel = *o*-phenanthroline (phen), 2,2′-bipyridyl (bpy)), prepared "in situ" from $[MnBr(chel)(CO)_3]$ and $AgClO_4$,[20] and 1,8-naphthyridine in a 1:1 molar ratio gave the complexes $[Mn(naph)(chel)(CO)_3]^+$ (chel = phen (**1**), bpy (**2**)).

The two new compounds are yellow solids and are very soluble in acetone. They decompose, when exposed to air, very slowly in the solid state but very readily in solution.

The analytical data are in accord with the proposed formulas, and the conductivity measurements show that both compounds are AB electrolytes. The IR ν(CO) vibration frequencies show that both complexes have a *fac* geometry with a symmetry lower than C_{3v} (E band split into two components). This geometry has been confirmed for the phen complex by an X-ray diffraction study. The ν(CO) band assignments were done in accord with those proposed for the analogous complexes *fac*-$[MnL_3(CO)_3]^+$ (L = aromatic amine).[21]

(17) Paudler, W. W.; Kress, T. J. *J. Org. Chem.* **1967**, *32*, 832.
(18) Wagner, J. R.; Hendricker, D. G. *J. Inorg. Nucl. Chem.* **1975**, *37*, 1375.
(19) Wooley, W. C. *J. Chem. Educ.* **1973**, *50*, A335 and references therein.
(20) Usón, R.; Riera, V.; Gimeno, J.; Laguna, M. *Transition Met. Chem. (London)* **1977**, *2*, 123.
(21) Bermejo, M. J.; Ruiz, J. I.; Vinaixa, J. *Transition Met. Chem. (London)* **1987**, *12*, 245.

Table II. Selected Bond Lengths (Å) and Angles (deg) for $[Mn(\eta^1\text{-naph})(\eta^2\text{-phen})(CO)_3]ClO_4 \cdot {}^1/_2CH_2Cl_2$ with Standard Deviations in Parentheses

Bond Lengths			
N(3)–Mn	3.199 (7)	C(2)–N(1)	1.356 (11)
N(1)–Mn	2.112 (7)	C(10)–N(1)	1.335 (12)
N(11)–Mn	2.040 (7)	N(3)–C(2)	1.372 (12)
N(20)–Mn	2.070 (6)	C(4)–N(3)	1.356 (13)
C(24)–Mn	1.848 (11)	O(24)–C(24)	1.117 (13)
C(25)–Mn	1.782 (10)	O(25)–C(25)	1.142 (12)
C(26)–Mn	1.790 (9)	O(26)–C(26)	1.148 (12)
Bond Angles			
N(11)–Mn–N(1)	87.0 (3)	N(20)–Mn–N(1)	88.0 (3)
N(20)–Mn–N(11)	79.5 (3)	C(24)–Mn–N(1)	94.4 (3)
C(24)–Mn–N(11)	173.5 (3)	C(24)–Mn–N(20)	94.2 (3)
C(25)–Mn–N(1)	175.2 (4)	C(25)–Mn–N(11)	89.0 (4)
C(25)–Mn–N(20)	93.9 (4)	C(25)–Mn–C(24)	89.8 (4)
C(26)–Mn–N(1)	91.2 (4)	C(26)–Mn–N(11)	96.2 (4)
C(26)–Mn–N(20)	175.6 (4)	C(26)–Mn–C(24)	90.2 (4)
C(26)–Mn–C(25)	86.6 (4)	C(2)–N(1)–Mn	125.8 (6)
C(10)–N(1)–Mn	118.7 (6)	C(10)–N(1)–C(2)	115.4 (7)
N(3)–C(2)–N(1)	114.5 (7)	C(7)–C(2)–N(1)	122.4 (8)
C(7)–C(2)–N(3)	123.0 (8)	C(4)–N(3)–C(2)	116.3 (8)
C(8)–C(7)–C(6)	124.3 (10)	O(24)–C(24)–Mn	173.8 (8)
O(25)–C(25)–Mn	176.8 (9)	O(26)–C(26)–Mn	178.7 (9)

Table III. Positional Parameters (×10⁴) for Non-Hydrogen Atoms with Estimated Standard Deviations in Parentheses

	x/a	*y/b*	*z/c*
Mn	1716 (1)	510 (10)	3855 (2)
Cl	−309 (1)	−2252 (2)	694 (3)
N(1)	2370 (4)	1366 (4)	5073 (9)
C(2)	2994 (4)	1660 (5)	4550 (11)
N(3)	3170 (4)	1404 (5)	3042 (10)
C(4)	3790 (5)	1686 (7)	2476 (13)
C(5)	4260 (5)	2198 (7)	3302 (14)
C(6)	4079 (6)	2424 (7)	4805 (15)
C(7)	3423 (5)	2175 (6)	5479 (12)
C(8)	3172 (6)	2452 (7)	6960 (12)
C(9)	2551 (5)	2192 (6)	7462 (13)
C(10)	2172 (5)	1643 (6)	6502 (12)
N(11)	1581 (4)	−60 (4)	6007 (9)
C(11)	1058 (5)	17 (6)	7065 (12)
C(12)	1018 (7)	−454 (7)	8464 (14)
C(13)	1520 (8)	−997 (8)	8795 (13)
C(14)	2086 (6)	−1099 (6)	7834 (12)
C(15)	2663 (8)	−1674 (8)	8033 (17)
C(16)	3160 (7)	−1771 (8)	6954 (16)
C(17)	3160 (5)	−1327 (6)	5500 (14)
C(18)	3630 (6)	−1416 (7)	4241 (19)
C(20)	3020 (5)	−434 (5)	2737 (12)
N(20)	2555 (3)	−308 (4)	3858 (9)
C(21)	2596 (5)	−753 (5)	5225 (11)
C(22)	3552 (5)	−978 (7)	2900 (16)
C(23)	2089 (5)	−634 (6)	6353 (11)
C(24)	1908 (4)	930 (6)	1852 (13)
O(24)	1979 (4)	1137 (5)	591 (9)
C(25)	1121 (5)	−217 (6)	2974 (11)
O(25)	714 (4)	−660 (5)	2435 (10)
C(26)	978 (5)	1194 (6)	4010 (13)
O(26)	497 (4)	1621 (5)	4095 (10)
O(1)	314 (6)	1476 (8)	182 (15)
O(2)	531 (6)	2093 (6)	−2209 (11)
O(3)	−384 (6)	2455 (8)	−751 (16)
O(4)	717 (9)	2831 (9)	78 (16)
C	4494 (15)	548 (16)	7640 (34)
Cl(1)	3563 (4)	364 (5)	8639 (11)
Cl(1)′	4186 (27)	183 (23)	8599 (53)
Cl(1)″	3502 (14)	456 (14)	8311 (28)
Cl(2)	4580 (7)	228 (9)	6143 (17)
Cl(2)′	4850 (8)	−296 (9)	7047 (21)
Cl(2)″	4801 (9)	−417 (10)	7973 (21)

Crystal Structure of *fac*-$[Mn(\eta^1\text{-naph})(\eta^2\text{-phen})(CO)_3]ClO_4 \cdot {}^1/_2CH_2Cl_2$. The crystal structure of *fac*-$[Mn(\eta^1\text{-naph})(\eta^2\text{-phen})(CO)_3]ClO_4 \cdot {}^1/_2CH_2Cl_2$ consists of discrete ions and solvate molecules linked by van der Waals and ionic forces. Figure 1

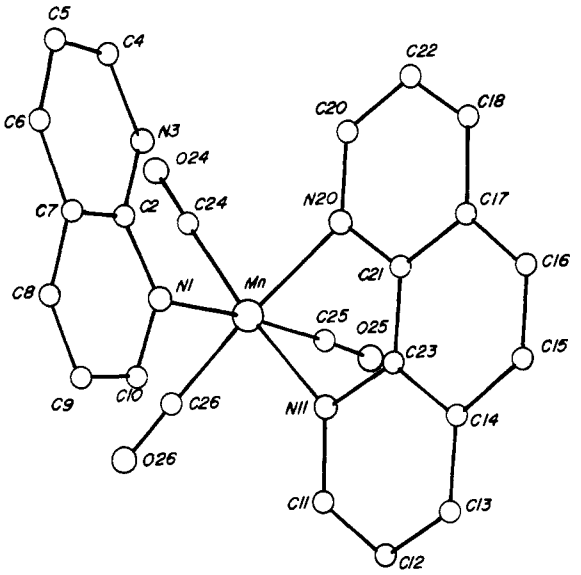

Figure 1. Molecular structure of *fac*-$[Mn(\eta^1\text{-naph})(\eta^2\text{-phen})(CO)_3]^+$ (cation of **1**).

shows a view of the complex ion with the atom numbering.

Selected bond distances and angles are given in Table II. Positional parameters for non-hydrogen atoms are listed in Table III.

The manganese atom displays a slightly distorted octahedral coordination, being linked to three carbon atoms of carbonyl ligands in a *fac* position and three nitrogen atoms, two from a bidentate *o*-phenanthroline ligand (η^2-phen) and one from a monodentate 1,8-naphthyridine ligand (η^1-naph).

The Mn–N(η^2-phen) bond distances [average 2.06 (1) Å] are similar to the Mn–N(phen) bond distances found in other octahedral complexes of Mn(I) with carbonyl ligands trans to the amine.[22]

The Mn–N(1)(η^1-naph) bond distance [2.112 (7) Å] is similar to that found in $[Mn(C_6H_4CH{=}N{-}N{=}CHPh)(CO)_4]$[23] but is significantly longer than that found for other Mn(I)–N(aromatic sp^2) bond lengths trans to a carbonyl ligand (2.04–2.06 Å)[22] or than that estimated[24] for a Mn–N(sp^2) single bond (2.07 Å). The lengthening of the Mn–N(1) bond is probably a consequence of the tendency of η^1-naph to minimize the Mn–N(3) contact. The Mn–N(3) distance of 3.199 (7) Å, much larger than the sum of the covalent radii of Mn(I) (1.39 Å)[25] and N(sp^2) (0.68 Å),[24] and the fact that there is very little distortion in the coordination of the η^1-naph ligand [bond angle C(25)–Mn–N(1) = 175.2 (4)°] are taken as indications that there is very little or no interaction between the manganese and the farthest nitrogen atom of the η^1-naph ligand.

The most important planes of the molecule and dihedral angles between them are listed in Table IV.

η^2-phen is almost coplanar with the equatorial plane (angle A/D). The plane of the η^1-naph ligand (plane E) is perpendicular to the equatorial plane (angle A/E) and splits the dihedral angle between the two axial planes (planes B and C) in such a way that the angle B/E is smaller than C/E. This configuration of the η^1-naph ligand is the one that minimizes the repulsions with the equatorial ligands, specially with the η^2-phen ligand.

Table IV. Dihedral Angles (deg) between the Most Important Planes

	Planes		
plane A (eq)	MnN(11)N(20)C(24)C(26)		
plane B (ax)	MnN(1)N(11)C(24)C(25)		
plane C (ax)	MnN(1)N(20)C(25)C(26)		
plane D (η^2-phen)	N(11)N(20)C(11–22)		
plane E (η^1-naph)	N(1)N(3)C(2–10)		
	Dihedral Angles		
A/B	87.8	A/C	88.4
A/D	2.9	A/E	83.3
B/C	84.5	B/D	84.9
B/E	38.7	C/D	88.4
C/E	57.05	D/E	80.9

Variable-Temperature ^{1}H NMR Study. The variable-temperature ^{1}H NMR spectra of both complexes are very similar, and only those of the *o*-phenanthroline complex, partly shown in Figure 2, are discussed.

$[Mn(\eta^1\text{-naph})(\eta^2\text{-phen})(CO)_3]^+$. In the whole range of temperature studied (233–348 K), the spectra of this complex showed the resonances of a symmetrically coordinated phen ligand. These resonances only experienced a small high-field shift on raising the temperature. At temperatures below 233 K viscosity broadening spoiled the experiment. The resonances of the naph ligand experienced, between 233 and 348 K, significant changes that merit a more detailed discussion. At temperatures between 233 and 273 K the spectra of the naph ligand consist of two broad doublets for the α-protons, two doublets of doublets for the β-protons, and another doublet of doublets for the γ-protons. These spectra may be interpreted by assuming that the two rings of the naph ligand are chemically nonequivalent and that the inter-ring couplings are small. Thus, the three protons of each ring, α, β, γ and α', β', γ', appear as two AMX spin systems. This supports a formulation in which only one nitrogen atom of the naph ligand interacts with the metal (structure I).

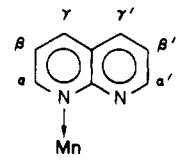

I

Thus, at low temperature the structure of the complex in solution is the same as that in the solid state: an octahedral Mn(I) complex of *fac* geometry with a bidentate phen and a monodentate naph ligand. Chemical shifts and coupling constants for the two compounds are listed in Table V. The coordinated (α, β, and γ) and noncoordinated (α', β', and γ') ring resonances were distinguished by use of the observation[8,14,15] that $J(\alpha\beta)$ is normally slightly increased on coordination to a metal atom and thus $J(\alpha\beta) > J(\alpha'\beta')$. Once these two coupling constants were assigned, the remaining assignments followed from the results of irradiation experiments and from mutual coupling relationships. All the protons of the amine are deshielded with respect to those of the free ligand. In the two complexes reported in this paper, the α-proton of the η^1-naph ligand appeared at higher field that the α'-proton. This had been previously observed in the square-planar complex *cis*-$[PtCl_2(\eta^1\text{-naph})(PPh_3)_2]$[8] but is the first time that such an observation has been reported for an octahedral complex. The expected behavior for the α-proton of a nitrogen heterocycle is a low-field shift of its ^{1}H NMR resonance on coordination, due to the descreening produced by the ligand to metal electron donation. Thus, for a monodentate 1,8-naphthyridine ligand the resonance of the α'-proton is expected at higher field than that of the α-proton. The anomalous behavior observed for the complexes $[Mn(\eta^1\text{-naph})(chel)(CO)_3]^+$ (chel = phen, bpy) can be explained in terms of a ring-current effect due to the electronic delocalization throughout the heterocyclic chelate ligand. As shown in the molecular structure of the phen complex discussed above, the α-proton of the η^1-naph ligand lies just above the

(22) (a) Carriedo, G. A.; Crespo, M. C.; Riera, V.; Valin, M. L.; Moreiras, D.; Solans, X. *Inorg. Chim. Acta* **1986**, *121*, 191. (b) Valin, M. L.; Moreiras, D.; Solans, X.; Font-Altaba, M.; Solans, J.; García-Alonso, F. J.; Riera, V.; Vivanco, M. *Acta Crystallogr., Sect. C* **1985**, *C41*, 1312. (c) Valin, M. L.; Moreiras, D.; Solans, X.; Font-Altaba, M.; García-Alonso, F. J. *Acta Crystallogr., Sect. C* **1986**, *C42*, 417. (d) Fayos, J.; Ulibarri, M. *Acta Crystallogr., Sect. B* **1982**, *B38*, 3086.
(23) Ceder, R. M.; Sales, J.; Solans, X.; Font-Altaba, M. *J. Chem. Soc., Dalton Trans.* **1986**, 1351.
(24) Little, R. C.; Doedens, R. J. *Inorg. Chem.* **1973**, *12*, 844.
(25) Cotton, F. A.; Richardson, D. C. *Inorg. Chem.* **1966**, *5*, 1851.

Table V. ^{1}H NMR Spectra of 1,8-Naphthyridine as the Free Compound and as a Ligand in $[Mn(naph)(chel)(CO)_3]^+$ (chel = phen (**1**), bpy (**2**))[a]

		chem shift, ppm[b]			coupling constant, Hz[b]		
compd	temp, K	α, α'	β, β'	γ, γ'	$\alpha\beta, \alpha'\beta'$	$\alpha\gamma, \alpha'\gamma'$	$\beta\gamma, \beta'\gamma'$
naph	308	8.97	7.47	8.28	4.1	2.0	8.2
1	273	9.21, 9.48	7.54, 7.85	8.58	5.05, 4.1	1.2	8.3, 8.0
	348	9.19	7.61	8.47	4.7	1.6	8.2
2	253	9.04, 9.39	7.66, *c*	*c*, *c*	5.2, 4.1	1.3, 1.8	8.1, *d*
	348	9.09	7.67	8.57	4.7	1.8	8.2

[a] In acetone-d_6. [b] α, β, and γ positions are labeled relative to the nitrogen atoms. Unprimed positions are adjacent to the coordinated nitrogen, and primed positions are adjacent to the noncoordinated nitrogen (see structure I in the text). [c] Overlapped with the resonances of the bpy ligand. [d] Not resolved.

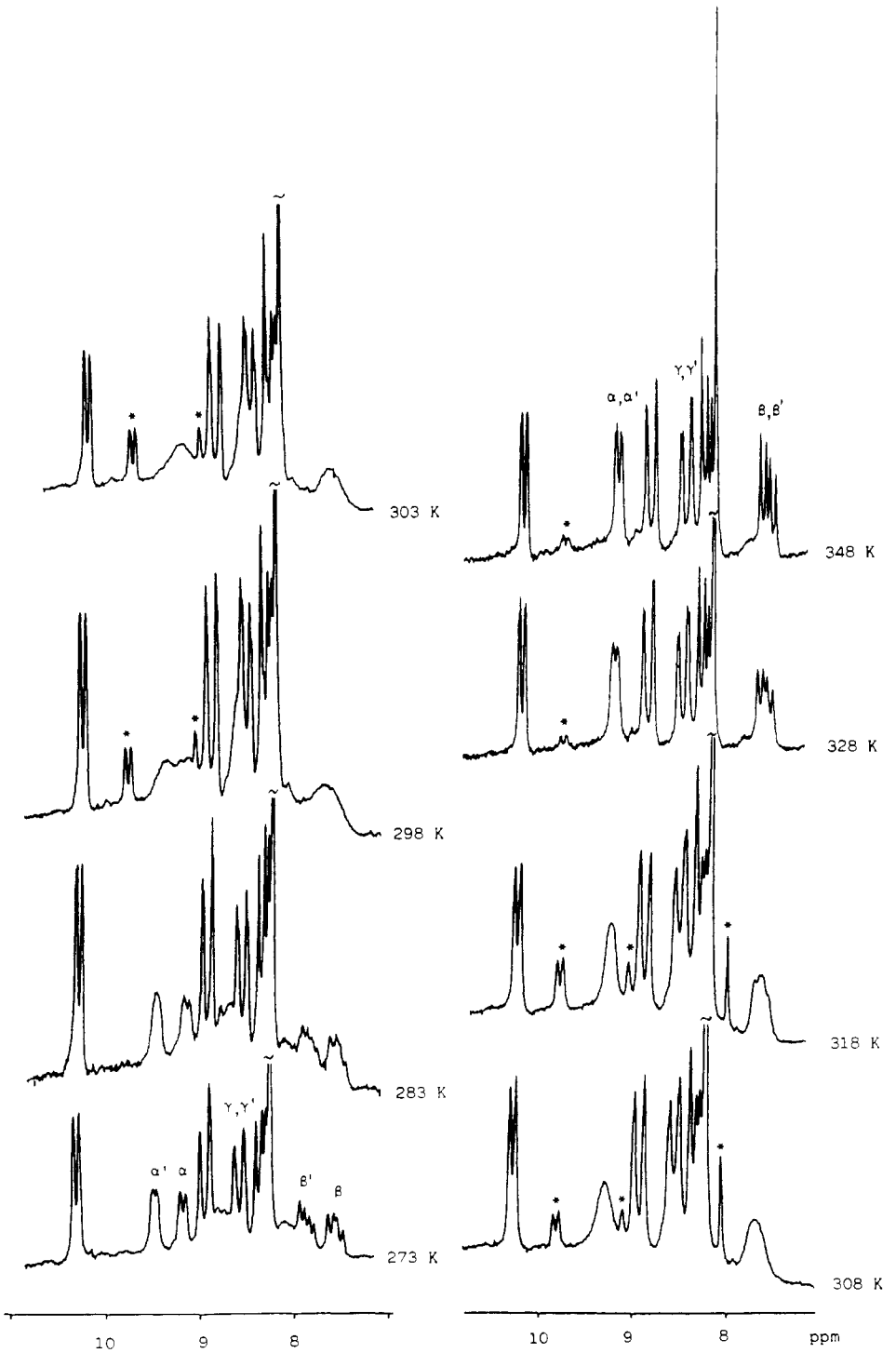

Figure 2. Variable-temperature ^{1}H NMR spectra (80 MHz) of $[Mn(naph)(phen)(CO)_3]^+$ (cation of **1**) in acetone-d_6. The peaks labeled α, β, γ, α', β', and γ' are those of the naph ligand and denote positions with respect to nitrogen atoms (see structure I in the text). The peaks marked with an asterisk are due to decomposition products.

equatorial plane of the complex (plane A). Free rotation of the η^1-naph ligand will result in the α-proton of that ligand spending a great deal of time in the shielding area above the chelate ligand, and so experiencing an upfield shift.

Warming the phen complex from 273 to 348 K caused a series of NMR changes illustrated in Figure 2. This results in a high-temperature-limit spectrum in which only a simple AMX pattern is distinguishible for the naph ligand, indicating that the α, β, γ and α', β', γ' nuclei are being rendered equivalent by a rapid metal exchange between the two nitrogen atoms in what can be called a 1,3-haptotropic shift.

From the coalescence of the α, α' and β, β' resonances of complex **1** and that of the α, α' resonances of complex **2** an approximate[26] energy barrier of 63 kJ/mol is obtained for the 1,3-haptotropic shift observed in both complexes. Although approximate, this value confirms our previous prediction[16] that, for octahedral complexes of first-row transition metals with an η^1-naph ligand, ΔG^* values for the intramolecular 1,3-haptotropic shift increase in the order Cr(0) {[Cr(η^1-naph)(CO)$_5$], 58.7 kJ/mol}[14] > Mn(I) {[Mn(η^1-naph)(η^2-chel)(CO)$_3$]$^+$ (chel = phen, bpy), 63 kJ/mol)} > Fe(II) {[Fe(η^1-naph)(CO)$_2$Cp]$^+$, $\gg$71 kJ/mol}.[15]

Mechanism of the Fluxional Process. In order to obtain information on the fluxional process, two different experiments were undertaken. First, the ^{1}H NMR spectra of acetone-d_6 solutions of complexes **1** and **2** at the coalescence temperature were obtained and no changes were observed when the samples were diluted first to half and then to one-fourth of the initial concentration. In the second experiment free naph was added to solutions of complexes **1** and **2** and their ^{1}H NMR spectra at 308 K were obtained: For both complexes the overlap between the α and β resonances of the free and coordinated 1,8-naphthyridine was very extensive, but the low-field doublet of the γ-proton of the coordinated naph ligand was clearly observed and not affected by the presence of free amine. These experiments showed that the 1,3-haptotropic shift was unimolecular, the only species involved being the complex itself. Thus, the mechanism for the fluxional exchange could either be intramolecular, involving a seven-coordinated manganese, or proceed through a 16-electron [MnL$_5$]$^+$/noninteracting 1,8-naphthyridine intermediate caught in the solvent cage. Our experimental results cannot distinguish between these two possible mechanisms. EH-MO calculations of the metal 1,3-haptotropic shift in the complex [Cr(η^1-naph)(CO)$_5$] have shown that the transition state contains substantial dissociative character, but due to the favorable orientation of the nitrogen lone pairs of the naphthyridine, some bonding interaction is still left.[27] According to that, we can speculate that for the naphthyridine complexes of manganese(I) reported in this paper the transition state for the 1,3-shift cannot be explained in terms of either a seven- or a five-coordinated manganese species but in terms of a concerted mechanism in which bond breaking is fundamental but some degree of interaction between the metal and the naphthyridine is kept throughout the reaction path.

Registry No. **1**, 116634-49-2; **2**, 116634-51-6; [MnBr(phen)(CO)$_3$], 56811-95-1; [MnBr(bpy)(CO)$_3$], 38173-71-6.

Supplementary Material Available: Tables of the crystal data collection and refinement, anisotropic thermal parameters and final hydrogen atom coordinates, all bond lengths and angles (hydrogen and non-hydrogen atoms), and the most important least-squares planes and deviations therefrom (10 pages); a listing of observed and calculated structure factors (9 pages). Ordering information is given on any current masthead page.

(26) Derived from the equation $\Delta G^* = 2.303RT_c(10.319 - \log k' + \log T_c)$, where T_c is the coalescence temperature and $k' = \pi(\Delta\nu)/2^{1/2}$: Calder, I. C.; Garrat, P. J. *J. Chem. Soc. B* **1967**, 660. $\Delta\nu$ is the frequency separation of the coalescing peaks, and the equation is strictly valid only for coalescence of two singlets. Consequently, the present results should be used only as an approximate indication of ΔG^*.

(27) Kang, S.-K.; Albright, T. A.; Mealli, C. *Inorg. Chem.* **1987**, *26*, 3158.

Contribution from the Department of Chemistry,
University of Houston—University Park, Houston, Texas 77204-5641

Dipalladium Complexes with *N,N'*-Diphenylbenzamidine Bridging and Chelating Ligands. Synthesis and Structural and Electrochemical Studies

C.-L. Yao, L.-P. He, J. D. Korp, and J. L. Bear*

Received May 12, 1988

The reaction of the palladium acetate trimer, Pd$_3$(OOCCH$_3$)$_6$, with lithium *N,N'*-diphenylbenzamidinate, Li(dpb), in CH_2Cl_2 gives a product with molecular formula Pd$_2$(dpb)$_4$. A single-crystal X-ray structure analysis shows the complex to contain two palladium(II) ions bridged by two dpb ligands, with an additional dpb ion chelated to each of the metals forming four-membered rings, [(dpb)Pd]$_2$(μ-dpb)$_2$ (**1**). Compound **1**, $C_{76}H_{60}N_8Pd_2\cdot H_2O\cdot CH_3OH$, crystallizes as large reddish orange parallelepipeds in space group $C2/c$ with 8 formula weights in a unit cell of dimensions a = 32.319 (7) Å, b = 22.396 (5) Å, c = 24.970 (5) Å, and β = 121.29 (1)°. Since there is no formal Pd···Pd bond, interligand repulsion of the bulky dpb molecules forces apart the the chelating groups, resulting in a dihedral angle between the two Pd(N)$_4$ coordination planes of 35° and a Pd···Pd separation of 2.90 Å. When **1** is refluxed in methanol, the two chelating ligands rearrange to form the tetrabridged complex, Pd$_2$(μ-dpb)$_4$ (**2**). Compound **2**, $C_{76}H_{60}N_8Pd_2\cdot C_2H_6O$, crystallizes as bright red columns in the orthorhombic space group *Pbca* with 8 formula weights in a unit cell of dimensions a = 22.230 (7) Å, b = 24.483 (9) Å, and c = 24.140 (9) Å. The Pd···Pd separation is 2.58 Å, and the two Pd(N)$_4$ coordination planes have an average torsion angle of 14.1°. The oxidation potentials of **1** and **2** show an effect on the HOMO's of the two molecules due to the proximity of the two palladium ions. Both of the two noninteracting palladium ions of **1** are oxidized irreversibly at 1.02 V vs SCE in CH_2Cl_2, 0.1 M TBAP, whereas under the same conditions **2** undergoes a reversible one-electron oxidation at 0.65 V to form the cation-radical complex [Pd^{II}Pd^{III}(μ-dpb)$_4$]$^+$. No other reversible cyclic wave was observed up to the potential limit of the solvent. The ESR spectrum of [Pd^{II}Pd^{III}(μ-dpb)$_4$]$^+$ clearly shows an axial signal with $g_\perp$ = 2.17 and $g_\parallel$ = 1.98. Satellite peaks due to ^{105}Pd ($I = {}^5/_2$, natural abundance 22.3%) are observed. The ESR spectrum is similar to that of the isoelectronic [Rh^{I}Rh^{II}(μ-dpb)$_4$]$^-$ complex and shows that the oxidation is metal centered.

Introduction

Among the dinuclear transition-metal complexes, the dirhodium compounds are the most sensitive to the nature of the axial and bridging ligands with respect to variation in their chemical and electrochemical behavior. This sensitivity is due, in a large part, to the high occupancy of the M–M antibonding molecular orbitals. Dirhodium(II) complexes with strong electron-pair-donor bridging ligands can be readily oxidized by two successive and reversible one-electron processes to produce the Rh^{II}Rh^{III} and Rh$^{III}_2$ oxidation states.[1-5] However, there are few examples of Rh$^{II}_2$ complexes

(1) Duncan, J.; Malinski, T.; Zhu, T. P.; Hu, Z. S.; Kadish, K. M.; Bear, J. L. *J. Am. Chem. Soc.* **1982**, *104*, 5507.
(2) Chavan, M. Y.; Zhu, T. P.; Lin, X. Q.; Ahsan, M. Q.; Bear, J. L.; Kadish, K. M. *Inorg. Chem.* **1984**, *23*, 4538.

0020-1669/88/1327-4389$01.50/0